The square root of mass as a fifth coordinate: geometry, stabilization, and spectral structure

Krzysztof Urbanowicz*
QWID Foundation
(Dated: July 15, 2026)

We develop a five-dimensional framework in which the square-root mass variable $\chi_m \equiv \sqrt{m}$ is represented by a dimensionful fifth coordinate $\xi = \kappa\chi_m$. The spacetime coordinates are $X^A = (t, x, y, z, \xi)$: no additional angular dimension is introduced. The Single Quantum Uncertainty Sphere (SQUS) is instead a spherical uncertainty structure in the ordinary three-dimensional spatial sector. In the canonical warped metric the physical size of every finite spatial separation scales as $|\xi|/L$ and therefore collapses at $\xi \to 0$. If the SQUS has no independent radial scale, self-similarity requires its coordinate radius to satisfy $R(\lambda\xi) = \lambda R(\xi)$, hence $R(\xi) \propto \xi$; combined with the canonical warp this gives the physical circumferential radius $f(\xi) \propto \xi^2$, providing a derivation of the quadratic horn scaling rather than an independent postulate. The pure quadratic horn produces an inner centrifugal barrier and a turning point, not by itself a stable circular orbit. For a general profile, a constant-ξ orbit requires $d\ln f/d\ln\xi = 1$, and linear stability requires the derivative of this logarithmic slope to be negative at the orbit. Consequently, stabilization of the absolute mass scale requires a separate radial well or a profile that crosses this condition; the Koide/equipartition potential fixes family direction but has a radial flat direction. The canonical five-dimensional geodesic calculation with $\xi \propto m^q$ retains the factor-of-two discriminator between $q = 1$ and $q = 1/2$, and the free-fall drift remains excluded by clock and ephemeris data. In the spectral sector, the concavity bound for operators $H_0 + \ell^2 U$ with $U \geq 0$ is unchanged; within the stated separable $U(1)$ winding ansatz, the simplest one-parameter evasion is a holonomy shift $\ell \to \ell - a$, which reproduces the normal-ordering neutrino ratios conditionally on the identification of the radial eigenvalue with $\sqrt{m}$. We separate exact results, model assumptions, and conditional phenomenology throughout.

I. INTRODUCTION

This paper develops the hypothesis that the variable $\chi_m \equiv \sqrt{m}$ underlies a fifth, mass-like coordinate. Because a spacetime coordinate must carry geometric units, we distinguish the mass variable from the dimensionful fifth coordinate,

$$\xi \equiv \kappa\chi_m = \kappa\sqrt{m}, \tag{1}$$

where the conversion constant κ fixes units. The five coordinates are therefore

$$X^A = (t, x, y, z, \xi), \tag{2}$$

and no additional angular coordinate is added to spacetime. Angular variables introduced below are ordinary spherical or azimuthal coordinates of the existing three-dimensional space. Three independent motivations converge on the square-root choice. First, a structural pattern of physics: linear quantities (field values, amplitudes) interfere and transform, while their squares (energies, probabilities) are positive and additive; mass behaves like the latter – it is variance-like – so the natural linear coordinate underneath it is $\sqrt{m}$, in exact analogy with the standard deviation underlying a variance. Second, an empirical motivation: the entire structure of the Koide relation for charged leptons – its equipartition formulation, its group theory, and its neutrino extension – lives in the variables $\sqrt{m_i}$, as shown in a companion paper [1] whose results we use throughout. Third, as shown in Sec. II, the measured distribution of fermion masses is log-uniform, the unique measure invariant under the reparametrization $m \leftrightarrow \chi_m$: the spectrum itself refuses to distinguish the two, so the question must be settled – and, we argue, is settled – by *angular* and *dynamical* structures, not by the radial measure.

The Koide relation [2, 3] and its precision (3×10^{-6} with current data [4]) motivate the flavor sector; the five-dimensional dynamics builds on the Space-Time-Matter program of Wesson and collaborators [5, 6], from which the present framework differs in exactly one place – the dictionary between the extra coordinate and mass – with consequences that are computed and confronted with data below.

Throughout we label claims by rigor: [A] theorems and exact computations, [B] computations confronted with data, [C] empirical regularities quoted with uncertainties but without mechanism, [D] hypotheses and outlook. Two of our central results are *no-go theorems* that kill natural readings of our own data (integer mass ladders, App. B 1; fractional spectral dimensions, App. B 2); we consider this pattern – hypotheses executed by their own theorems – the methodological core of the paper.

The paper is organized as follows. Section II develops the kinematics of the mass dimension: the master decomposition $m = \bar{\chi}_m^2 + \mathrm{Var}(\chi_m)$, the factorization of transitions, and the fixed-point measure. Sec-

* krzysztof.urbanowicz@qwid.org

TABLE I. Phenomenological benchmarks for the decomposition (3); the displacement/variance fractions are model interpretations. $\lambda_C = \hbar/mc$ is the irreducible spatial extent; $\sigma \sim m^3c^4/\hbar^2$ and $P \sim m^4c^5/\hbar^3$ are the Madelung anti–surface-tension and kinematic pressure evaluated at the Compton scale. The lightest-neutrino mass is the equipartition-cone prediction of [1].

Mode	m	$\bar{\chi}_m^2$ frac.	λ_C	σ [N/m]
ν_1 (cone)	0.364 meV	~ 1	0.54 mm	2.4×10^{-17}
electron	0.511 MeV	~ 1	3.9×10^{-13} m	6.6×10^{10}
proton	938 MeV	~ 0.01	2.1×10^{-16} m	4.1×10^{20}
top	172.6 GeV	~ 1	1.1×10^{-18} m	2.5×10^{27}

tion III performs the Wesson calculation with the $\sqrt{m}$ dictionary and its double exclusion by data, deriving the stabilization requirement. Section IV develops the five-dimensional SQUS geometry, derives the quadratic horn scaling from a single-scale assumption, and distinguishes an inner centrifugal barrier from genuine orbital stability before demolishing the integer-ladder alternatives. Section V contains the spectral sector: the concavity no-go theorem and its resolution by a $U(1)$ holonomy/rotation, with its prediction menu. Section VI compares three distinct manifestations of scale-invariant structure without assuming a common microscopic origin. Section VII bridges to the flavor results of [1]. Section VIII reports a negative cosmological result and a conjecture. Section IX collects the dated falsifiers, and Sec. X concludes.

II. KINEMATICS OF THE MASS DIMENSION

A. The master decomposition [A/D]

For any operator-valued variable χ_m with finite variance, the identity

$$m \;\equiv\; \langle \chi_m^2 \rangle \;=\; \bar{\chi}_m^2 + \mathrm{Var}(\chi_m) \tag{3}$$

is exact once the model defines the observed mass by $m = \langle \chi_m^2 \rangle$ [A]. The further identification of the first term with Higgs-type mass generation and of the second with condensate/fluctuation energy is a physical interpretation [D], not a Standard-Model theorem: the Higgs field is not literally χ_m, and QCD mass is not automatically a statistical variance of this operator. We nevertheless use the decomposition as a bookkeeping ansatz and list limiting phenomenological examples in Table I. The top quark is a useful near-displacement benchmark because it decays before hadronizing, while the proton is a useful fluctuation-dominated benchmark; these labels should be read as model interpretations rather than unique observable partitions of a measured mass.

Two immediate consequences of the coordinate reading are worth recording. Mass changes factorize,

$$\Delta m = \chi_{m,f}^2 - \chi_{m,i}^2 = \Delta\chi_m\,(\chi_{m,i} + \chi_{m,f}), \tag{4}$$

so the energy released in a transition is a geometric step times the sum of positions – the same objects, sums and differences of $\sqrt{m}$, out of which the Koide ratio is built. And dimensionally $[m] = [1/t]$ implies $[\chi_m] = [1/\sqrt{t}]$: the mass axis is an axis of clock frequencies, one Compton period corresponding to exactly one quantum of action, $mc^2\,T_C = h$. Time–energy uncertainty then makes stability and sharpness equivalent on the axis: a resonance of width Γ is delocalized by $\Delta\chi_m = \Gamma/(2c^2\sqrt{m})$ (0.41% of $\bar{\chi}_m$ for the top quark), while an absolutely stable mode is a mathematical point.

B. The measure is a fixed point [B]

Is the spectrum of masses distributed uniformly in m, in χ_m, or in $\ln m$? A maximum-likelihood fit of a truncated power law $\rho(m) \propto m^{-\gamma}$ to the nine charged-fermion masses gives

$$\gamma = 1.044 \pm 0.091, \tag{5}$$

i.e. log-uniformity; uniformity in χ_m ($\gamma = \frac{1}{2}$) is disfavored by $\Delta \ln L = -14.7$ and uniformity in m by -25.1. Within the power-law family, the log-uniform measure is the fixed point of the substitution $m = \chi_m^2$ ($\rho \propto 1/m \mapsto \rho \propto 1/\chi_m$): nature populated the mass axis with precisely the distribution that carries no information about which power of mass is fundamental. The radial measure is silent about the coordinate; the evidence for χ_m presented below is angular (Secs. IV–V) and dynamical (Sec. III).

III. FIVE-DIMENSIONAL DYNAMICS: THE WESSON CALCULATION WITH $\xi \propto \sqrt{m}$

A. Geodesics and the dictionary [A]

We adopt the canonical metric of Space-Time-Matter theory [5, 7], written for the dimensionful fifth coordinate ξ,

$$dS^2 = \frac{\xi^2}{L^2}\, g_{\mu\nu}(x)\, dx^\mu dx^\nu - d\xi^2, \qquad L = \sqrt{3/\Lambda}. \tag{6}$$

Let $ds^2 = g_{\mu\nu}dx^\mu dx^\nu$ be the four-dimensional proper interval. Along a null five-dimensional curve,

$$0 = \frac{\xi^2}{L^2} ds^2 - d\xi^2, \tag{7}$$

so, when parametrized by s,

$$\frac{d\xi}{ds} = \pm\frac{\xi}{L}. \tag{8}$$

This relation uses the four-dimensional proper interval directly and does not require a separate normalization of the warped 4D term.

The geometry is identical to the canonical Wesson sector; the physics enters through the dictionary

$$\xi = \kappa m^q. \tag{9}$$

Equation (8) gives $|\dot{m}/m| = 1/(qL)$ in units with $c = 1$ (or $c/(qL)$ for coordinate time). Thus the square-root choice $q = 1/2$ doubles the secular rate relative to $q = 1$:

$$\left|\frac{\dot{m}}{m}\right| = \begin{cases} 5.7 \times 10^{-11}\,\mathrm{yr}^{-1} & q = 1 \text{ (Wesson)}, \\ 1.15 \times 10^{-10}\,\mathrm{yr}^{-1} & q = \frac{1}{2} \text{ (this work)}, \end{cases} \tag{10}$$

for the numerical value of L used here. The conversion constant κ cancels from the relative drift but remains relevant for any absolute geometric radius.

B. The causal budget [A/D]

The null condition also gives a useful kinematic identity. In a local frame of the ordinary three-dimensional spatial sector,

$$v_3^2 + w_\xi^2 = c^2, \qquad w_\xi \equiv L\,\frac{d\ln\xi}{dt}, \tag{11}$$

where $v_3^2 = \dot{x}^2 + \dot{y}^2 + \dot{z}^2$ locally. Hence $v_3 \le c$ identically. No extra angular velocity is added to this budget: an azimuthal SQUS circulation is part of the ordinary three-velocity v_3, because its angle is an ordinary spatial coordinate.

For a local orthogonal decomposition of the ordinary spatial motion into a center-of-mass part and an internal circular part one may write, as an effective kinematic ansatz [D],

$$v_{\mathrm{cm}}^2 + v_{\mathrm{circ}}^2 + w_\xi^2 = c^2. \tag{12}$$

A stabilized mode at center-of-mass rest then admits $v_{\mathrm{circ}} = c$; this is the zitterbewegung-like reading used below. Because the decomposition is internal to the existing three-space, it must not be interpreted as a sixth dimension. The robust [A] statement is Eq. (11); the identification of a particular share with an internal Compton circulation is a model hypothesis [D].

Scale travel remains cosmologically slow: a mode at spatial rest using its entire null budget in the fifth direction obeys $d\ln\xi/dt = c/L$, i.e. one e-fold per L/c. The observational bounds below therefore constrain any residual leakage along the fifth coordinate.

C. Double exclusion [B]

Only dimensionless quantities are observable [8], and the two judges are $\mu \equiv m_p/m_e$ and the ephemeris products GM. If the drift affects the coordinate (Higgs) component of masses while Λ_{QCD} is fixed by dimensional transmutation, then, with the proton sigma-term fraction $f_\sigma \approx 0.06$,

$$\frac{\dot{\mu}}{\mu} \approx 2v\,(f_\sigma - 1) \approx -1.9\,v, \qquad v \equiv \frac{\dot{\xi}}{\xi}, \tag{13}$$

and the geodesic rate violates the clock and quasar bound $|\dot{\mu}/\mu| \lesssim 5\times10^{-17}\,\mathrm{yr}^{-1}$ [9, 10] by a factor 2×10^6; the same quasar spectroscopy enforces the *spatial* homogeneity of the fifth-coordinate/SQUS structure (identical radial completion and holonomy data over every base point) at the 10^{-5}–10^{-7} level, so that a position-dependent a would show up as neutrino mass ratios varying across the sky. If instead the drift is universal, dimensionless mass ratios are constant but the measured GM of celestial bodies (in atomic units) drifts at the same rate, violating $|d(GM)/dt|/GM \lesssim 10^{-13}\,\mathrm{yr}^{-1}$ [11] by three orders of magnitude. A compensation by co-varying couplings is not an escape: complete compensation is a units redefinition [8], and partial compensation must silence every dimensionless judge (α, μ, $Gm_p^2/\hbar c$, $m_q/\Lambda_{\mathrm{QCD}}$) simultaneously, without a mechanism. Table II summarizes.

TABLE II. Confrontation of the free-fall (null-geodesic) mass drift with data. Both dictionaries are excluded in both scenarios: the failure is not the choice of q but the assumption of free fall along ξ.

Scenario	Judge	Limit [yr^{-1}]	Excess ($q = \frac{1}{2}$)
differential	$\dot{\mu}/\mu$	5×10^{-17}	$\times 2 \times 10^6$
universal	$d(GM)/dt/GM$	1×10^{-13}	$\times 10^3$

D. The stabilization requirement [A/B]

Particles therefore cannot fall freely along the mass direction: the residual velocity in ξ must be strongly suppressed relative to the free null-geodesic rate. This requires stabilization of the *absolute scale*. The equipartition potential of the companion paper,

$$V_{\mathrm{eq}} = (n_{\mathbf{1}} - n_{\mathbf{2}})^2, \tag{14}$$

fixes the family direction $Q = 2/3$ but has an exact radial flat direction: on the Koide cone, $V_{\mathrm{eq}} = 0$ for every common rescaling $\chi_{m,i} \to \lambda\chi_{m,i}$. It therefore cannot by itself stop a common drift of all masses.

A complete stabilization sector must separate scale from flavor, for example

$$V_{\mathrm{tot}} = V_{\mathrm{rad}}(\rho) + V_{\mathrm{eq}}, \qquad \rho^2 \equiv \sum_i \chi_{m,i}^2, \tag{15}$$

where V_{rad} fixes the overall mass scale and V_{eq} fixes the angular position in family space. The SQUS geometry developed in Sec. IV supplies a natural inner barrier and can contribute to V_{rad}, but the pure quadratic horn is not by itself a stable circular well. The observational drift bound should therefore be interpreted as a bound on leakage from whatever radial completion realizes the minimum [D].

IV. SQUS GEOMETRY, HORN SCALING, AND RADIAL STABILITY

A. Five dimensions, no extra angular coordinate [A/D]

The SQUS construction remains five-dimensional. The coordinates are

$$X^A = (t, x, y, z, \xi), \tag{16}$$

or equivalently $(t, r, \vartheta, \varphi, \xi)$ when the ordinary three-space is written in spherical coordinates. The angles ϑ and φ are therefore not extra dimensions. At fixed time the canonical spatial interval is

$$d\ell_3^2 = \frac{\xi^2}{L^2}\left(dr^2 + r^2 d\Omega^2\right), \qquad d\Omega^2 = d\vartheta^2 + \sin^2\vartheta\, d\varphi^2. \tag{17}$$

Every finite coordinate separation has proper size proportional to $|\xi|/L$ and therefore collapses metrically as $\xi \to 0$. The locus $\xi = 0$ is thus the common degenerate tip at which every finite coordinate separation in the ordinary spatial section has zero proper length, not an internal circle appended to spacetime.

Let $R(\xi)$ denote the coordinate-space radius of the SQUS orbit in the ordinary three-space. Its physical circumferential radius is

$$f(\xi) = \frac{|\xi|}{L} R(\xi). \tag{18}$$

The "single" in SQUS is implemented by the absence of an independent radial scale: under a rescaling of the only geometric scale, $\xi \to \lambda\xi$, the coordinate radius obeys

$$R(\lambda\xi) = \lambda R(\xi). \tag{19}$$

For a differentiable positive profile this homogeneity condition gives $\xi R'(\xi) = R(\xi)$ and hence $R(\xi) = \alpha\xi$. Combining this with Eq. (18) yields

$$\boxed{f(\xi) = \frac{\xi^2}{R_s}, \qquad R_s \equiv \frac{L}{\alpha}.} \tag{20}$$

Thus one factor of ξ comes from the canonical five-dimensional warp and the second from the single-scale SQUS radius. In mass variables, using $\xi = \kappa\sqrt{m}$, the same statement is $f = (\kappa^2/R_s)m$.

If the SQUS is represented explicitly as the embedded family $r = R(\xi)$, its induced radial coefficient is

$$B(\xi) = 1 + \frac{\xi^2}{L^2}[R'(\xi)]^2 > 0. \tag{21}$$

This factor can be absorbed locally into a proper radial coordinate and does not change the constant-orbit conditions below.

B. Barrier versus stable orbit [A]

Restricting the five-dimensional geometry to an adapted SQUS sector, with φ an ordinary azimuthal angle, gives the reduced line element

$$dS_{\rm red}^2 = \frac{\xi^2}{L^2}(dt^2 - dz^2) - B(\xi)d\xi^2 - f(\xi)^2 d\varphi^2. \tag{22}$$

No new spacetime coordinate has been introduced: φ replaces an ordinary Cartesian spatial coordinate in the adapted description. For a null trajectory with conserved quantities $E = (\xi/L)^2\dot{t}$, $p = (\xi/L)^2\dot{z}$, and $J = f^2\dot{\varphi}$, one obtains

$$B(\xi)\dot{\xi}^2 = \frac{A}{\xi^2} - \frac{J^2}{f(\xi)^2}, \qquad A = L^2(E^2 - p^2). \tag{23}$$

After using proper radial distance one may set $B = 1$ locally. Define $F(\xi) = A/\xi^2 - J^2/f(\xi)^2$. A constant-$\xi$ circular orbit requires both $F(\xi_*) = 0$ and $F'(\xi_*) = 0$, not merely $\dot{\xi} = 0$. Introducing

$$h(\xi) \equiv \frac{d\ln f}{d\ln\xi} = \frac{\xi f'(\xi)}{f(\xi)}, \tag{24}$$

the orbit condition is

$$\boxed{h(\xi_*) = 1.} \tag{25}$$

Linearizing about the orbit gives $F''(\xi_*) = 2Ah'(\xi_*)/\xi_*^3$, so stability requires

$$\boxed{h'(\xi_*) < 0.} \tag{26}$$

The pure quadratic horn of Eq. (20) has $h = 2$ everywhere and therefore has no constant-radius circular orbit. Instead,

$$\dot{\xi}^2 = \frac{A}{\xi^2} - \frac{J^2 R_s^2}{\xi^4} \tag{27}$$

has a turning point at

$$\boxed{\xi_t^2 = \frac{J^2 R_s^2}{A},} \tag{28}$$

where, for $B = 1$, $\ddot{\xi} = A/\xi_t^3 > 0$. The quadratic horn therefore provides an inner centrifugal barrier and reflection from the tip, not a self-sufficient stable orbit.

A genuine geometric stabilizer must retain the quadratic behavior near the tip while crossing $h = 1$ with negative slope. One explicit example is

$$f_{\rm stab}(\xi) = \frac{\xi^2/R_s}{1 + (\xi/\xi_c)^2}, \tag{29}$$

for which $h = 2/[1 + (\xi/\xi_c)^2]$, so $h(\xi_c) = 1$ and $h'(\xi_c) < 0$. The additional balance condition $F(\xi_c) = 0$ selects the conserved-quantity combination of the circular mode.

This profile is only an explicit example; equivalently, a separate $V_{\rm rad}$ in Eq. (15) may fix the scale.

Figure 1 summarizes the revised geometric and dynamical logic. Panel (a) compares the physical SQUS circumferential radius in ordinary three-space for a linear reference, the single-scale quadratic horn, and one explicit stabilizing completion. Panel (b) displays the logarithmic slope $h = d\ln f/d\ln\xi$: the pure quadratic horn remains at $h = 2$ and therefore never satisfies the constant-radius condition, whereas the completed profile crosses $h = 1$ at $\xi = \xi_c$ with $h'(\xi_c) < 0$. Panel (c) shows the corresponding radial function $F(\xi) = \dot{\xi}^2$. The zero of the pure quadratic horn is a turning point ξ_t, while the completed profile is tuned to satisfy both $F(\xi_c) = 0$ and $F'(\xi_c) = 0$, giving the constant-ξ solution. The normalization used in the figure is schematic; only the qualitative relations and the distinguished points ξ_t and ξ_c are used in the argument.

C. Zitterbewegung identification [D]

The circulation, when invoked, takes place in the ordinary three-dimensional SQUS geometry. A light-speed circular mode with momentum $p = mc$ at the reduced Compton radius $R = \hbar/(mc)$ carries $E = pc = mc^2$, so the rest energy can be represented kinematically as circulation energy in the spirit of zitterbewegung [12, 13] and Penrose's zigzag [14]. For the cone neutrino ν_1 the reduced Compton radius is $R_1 = 0.542$ mm. This identification is a model hypothesis, not a derivation of spin. In fact, $pR = \hbar$ for the stated radius, whereas a spin-1/2 assignment requires additional spinorial or half-angle structure; the present scalar SQUS geometry does not yet supply that step.

D. Refuted alternatives [A/B]

Honesty requires demolishing the natural ladder readings of our own numbers. A shared-radius tower, $m_n \propto n$, is refuted by the cone spectrum itself (mass ratios $1 : 23.80 : 137.72$). Exact integer ladders in χ_m are refuted by a theorem: *no integer triple* $(1, a, b)$ *lies on the equipartition cone, in either sign class* (App. B 1; a brute-force scan to 3000 confirms). The tempting reading $\chi_m \propto (1, 5, 12)$ gives $Q = 170/256 = 0.66406$ (angle 44.888°), off the cone by 0.4%; it fits the measured Δm^2 ratio equally well (-0.36σ) with $m_1 = 0.3465$ meV, but predicts $\Sigma m_\nu = 58.90$ meV versus the cone's 59.16 meV – a 0.26 meV discriminator for far-future cosmology. The proximity of $m_3/m_1 = 137.7$ to $1/\alpha$ carries no information: the ratio's uncertainty ($\sim \pm 2$) covers several integers.

V. SPECTRAL SECTOR: WAVE TOWER, NO-GO, AND FLUX

A. Consecutive winding modes [B]

Treat the three normal-ordering cone neutrinos [1, 15, 16] as consecutive standing-wave levels $\ell = 1, 2, 3$ around the ordinary-space SQUS azimuthal loop, with radial closure supplied by a stabilizing completion of the geometry. The data are two dimensionless ratios (Monte-Carlo propagated from Δm^2),

$$r_2 \equiv \frac{\chi_{m,2}}{\chi_{m,1}} = 4.878 \pm 0.044, \qquad r_3 \equiv \frac{\chi_{m,3}}{\chi_{m,1}} = 11.737 \pm 0.182. \tag{30}$$

One-parameter spectral families fitted to r_2 then *predict* r_3: towers in the *mass* ($m \propto \lambda_\ell$) fail at -14 to -16σ, towers in χ_m pass at -0.3 to -0.6σ – a further independent discriminator, alongside the flavor sector of [1], that the wave variable is $\sqrt{m}$, not m. The formal fit $\chi_m \propto \ell(\ell + d - 1)$ returns $d_{\rm eff} = 0.695$; we now show this parametrization has no geometric realization.

B. A concavity no-go theorem [A]

For any effective SQUS profile $f(\xi)$ and any self-adjoint radial closure, the azimuthal quantum number enters the radial problem as $\ell^2\, U(\xi)$ with $U \geq 0$. The lowest eigenvalue of $H_0 + \lambda U$ is concave in $\lambda = \ell^2$ (an infimum of linear functions), and concavity with $\varepsilon(0) \geq 0$ gives (App. B 2)

$$\frac{\varepsilon_2}{\varepsilon_1} \leq 4, \qquad \frac{\varepsilon_3}{\varepsilon_1} \leq 9. \tag{31}$$

The data exceed these bounds by $+20\sigma$ and $+15\sigma$. Numerical scans of horn powers $N = 1.5, 2, 3$ with a Dirichlet closure approach but never exceed the bounds (max ratios 3.5–4.0 and 7.1–9.0). The fractional-dimension reading is therefore excluded within this scalar separable SQUS operator class: no profile of the stated form realizes the neutrino tower without an additional shift or structure. We record this as the second instance of a hypothesis executed by its own theorem.

C. Resolution: holonomy, equivalently rotation [B/D]

Within the separable one-parameter $U(1)$ winding ansatz, the simplest modification that evades Eq. (31) shifts ℓ instead of scaling it. A $U(1)$ holonomy around the closed SQUS loop gives an Aharonov–Bohm phase a in units of the flux quantum [17]. No compact extra angular dimension is required: the holonomy is associated with a closed path in the ordinary spatial sector,

$$\varepsilon_\ell \;\propto\; (\ell - a)^2. \tag{32}$$

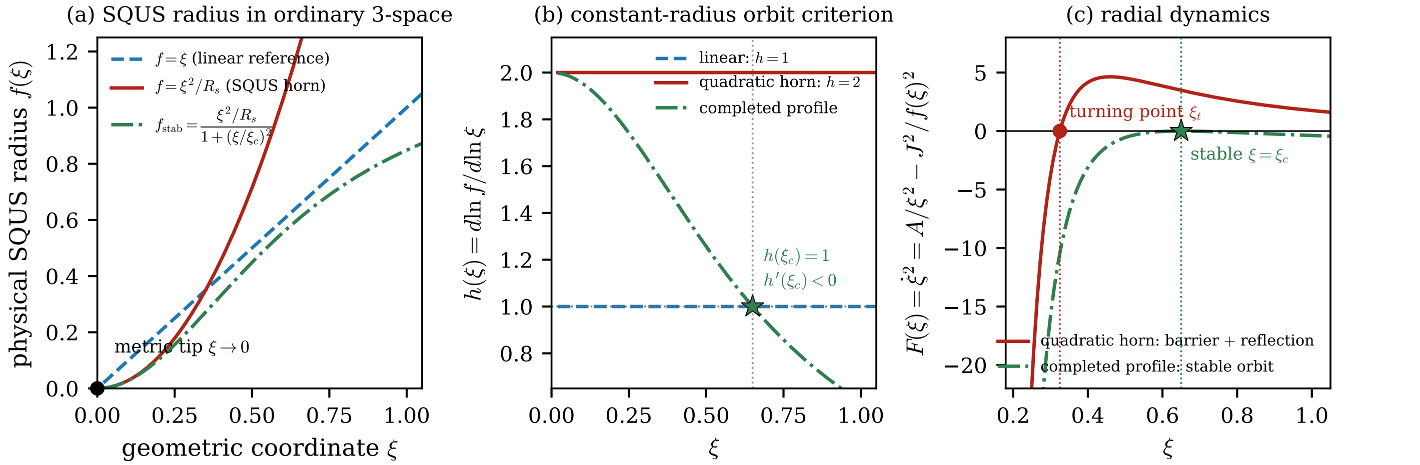

FIG. 1. Revised SQUS geometry and radial dynamics in the existing three-dimensional spatial sector. **(a)** Physical SQUS radius $f(\xi)$. The dashed line is a linear reference, the red curve is the single-scale quadratic horn $f = \xi^2/R_s$ derived from the canonical warp, and the green curve is the explicit completion $f_{\text{stab}} = (\xi^2/R_s)/[1 + (\xi/\xi_c)^2]$, which preserves the quadratic tip behavior. **(b)** Logarithmic slope $h(\xi) = d\ln f/d\ln\xi$. A constant-ξ orbit requires $h = 1$; linear stability requires a negative crossing, $h'(\xi_*) < 0$. The pure quadratic horn has $h = 2$ everywhere and therefore cannot by itself support such an orbit, whereas the completed profile satisfies $h(\xi_c) = 1$ and $h'(\xi_c) < 0$. **(c)** Radial function $F(\xi) = A/\xi^2 - J^2/f(\xi)^2$. For the quadratic horn, the root $\xi_t^2 = J^2R_s^2/A$ is a turning point associated with centrifugal reflection. For the completed profile, the conserved quantities are chosen so that $F(\xi_c) = F'(\xi_c) = 0$, yielding the stable constant-ξ solution shown by the star. Numerical normalizations in all three panels are illustrative.

Fitting a to r_2 gives

$$a = 0.1726 \pm 0.0068, \qquad r_3^{\text{pred}} = 11.678 \ \ (-0.3\sigma), \quad (33)$$

with the candidate values $\pi/18$ (-0.28σ) and $1/6$ $(+0.87\sigma)$ both viable [C] and undiscriminated (a look-elsewhere caveat applies). Equation (32) is algebraically the $(\ell+\alpha)^2$ family of the tower fit; what is new is its geometric realizability within the stated separable $H_0 + \ell^2U$ class. Other mechanisms outside this class are not excluded by the theorem.

By the Sagnac–Aharonov–Bohm equivalence [19], the identical stationary spectrum can also arise from a *rotating* SQUS background: an ordinary-space loop rotating at angular velocity Ω gives, in the co-rotating frame, $E_\ell \propto (\ell - I\Omega/\hbar)^2 + \text{const}$. In this reading a is a measurement of the sphere's angular momentum, $L_{\text{SQUS}} \approx 0.17\,\hbar$ per mode. We state the epistemic limit explicitly: the stationary spectrum cannot distinguish flux from rotation; only time-dependent (Sagnac-precession) effects could.

D. The full spectrum and its prediction menu [B/D]

Table III and Fig. 2 display the full winding spectrum. Beyond reproducing $\nu_{1,2,3}$, the algebraic continuation of the same spectrum contains a candidate level at $\ell = 4$,

$$m_4 = 166.7 \text{ meV}, \quad (34)$$

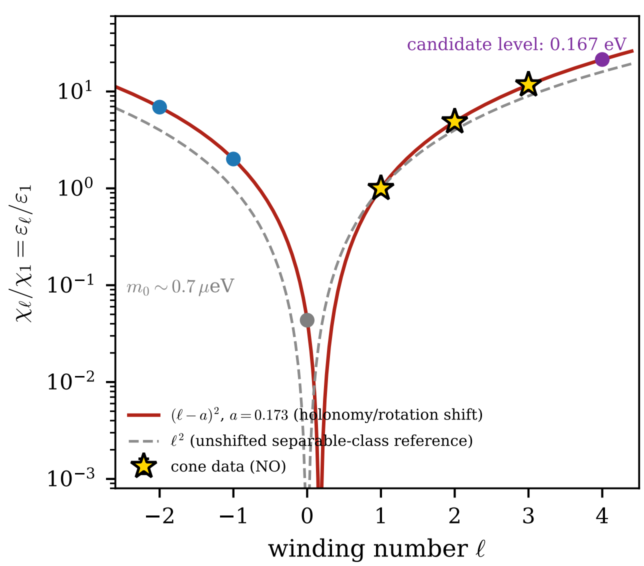

FIG. 2. The winding spectrum $(\ell - a)^2$ with $a = 0.173$ (solid) against the flux-free bound ℓ^2 (dashed), which no operator in the stated scalar separable $H_0 + \ell^2U$ class can exceed. Stars: the equipartition-cone ratios with uncertainties. Circles: model levels, including formal counter-rotating levels $\ell < 0$, the near-zero $\ell = 0$ level, and the candidate extra level $\ell = 4$.

a near-zero level at $\ell = 0$, $m_0 \approx 0.7\,\mu$eV, and a counter-rotating branch $\ell = -1, -2$ at 1.47 and 17.3 meV. These are *conditional level locations*, not yet complete exper-

TABLE III. The winding spectrum $\varepsilon_\ell \propto (\ell - a)^2$, $a = 0.1726$, normalized to $\ell = 1$; masses from $m_\ell = m_1(\chi_{m,\ell}/\chi_{m,1})^2$ with $m_1 = 0.364$ meV.

ℓ	$\chi_{m,\ell}/\chi_{m,1}$	m_ℓ [meV]	role
0	0.044	6.9×10^{-4}	formal near-zero level
1	1.000	0.364	ν_1
-1	2.009	1.468	formal counter-rotating
2	4.878	8.661	ν_2
-2	6.895	17.31	formal counter-rotating
3	11.678	49.64	ν_3
4	21.399	166.7	candidate extra level

imental predictions: the present model does not determine the mixing matrix, production rate, thermalization history, or whether every formal branch is populated. In particular, a reactor test of the $\ell = 4$ level requires a nonzero $|U_{e4}|^2$, which is not predicted here. Rotation can split co- and counter-rotating branches, and more elaborate rotating backgrounds may exhibit instabilities [20, 21], but the present framework does not yet derive a quantitative instability criterion. Absence of a branch therefore cannot be counted as a falsifier until such a criterion is supplied. We note honestly that with three masses (two dimensionless numbers) the curve fit alone has weak selective power; the strength of this section lies in the restricted-class no-go theorem and in the conditional spectral fit, not in a claim of absolute uniqueness.

VI. SELF-SIMILARITY AND CRITICALITY

In quantum field theory mass is associated with an inverse correlation length. We therefore explore [D] the possibility that the tip $\xi = 0$ corresponds to a critical limit and that scale transformations along the mass variable, $\chi_m \to \lambda\chi_m$, encode an RG-like self-similarity. The A/ξ^2 term of Eq. (23) is scale free, while the SQUS barrier or a radial completion introduces a scale.

Three distinct observations exhibit related scale-invariant structure; we do not claim that a common microscopic measure has yet been derived. (i) The fermion mass spectrum: $\gamma = 1.044 \pm 0.091$ (Sec. II). (ii) The Koide ratio is frozen from M_Z to the GUT scale at the 10^{-6} level [1]: the ratio is numerically quasi-invariant across a wide energy range in the stated running analysis. (iii) The electron itself: computing the one-loop Källén–Lehmann mass budget of the dressed electron and projecting on shell gives the closed form

$$\frac{d(\delta m)}{d\ln s} = \frac{\alpha m}{4\pi}\,\frac{3s - m^2}{s}, \tag{35}$$

whose ultraviolet plateau equals the RG anomalous dimension *exactly*, $\gamma_m = 3\alpha/2\pi$ per e-fold of scale ($3\alpha/\pi = 0.697\%$ per e-fold of χ_m): the spectral dressing profile and the RG flow are one function (Fig. 3). In the particular one-loop on-shell bookkeeping used here, integration to the Planck scale assigns 18.7% to multi-scale dressing and roughly 81% to the pole term; this split is scheme-dependent and should not be read as a unique observable mass budget. The infrared cloud is the empirical $1/\omega$ bremsstrahlung spectrum, log-uniform again, while the mass budget is infrared-finite – reconciling self-similarity with the sharpness $\Delta\chi_m \to 0$ of a stable particle (the infraparticle structure [23] resides in the normalization, not the mass). In the oldest language available: a particle that lasts forever is a fixed point of aggregation-and-rescaling, the same structure that makes the Gaussian indestructible in the central limit theorem [24].

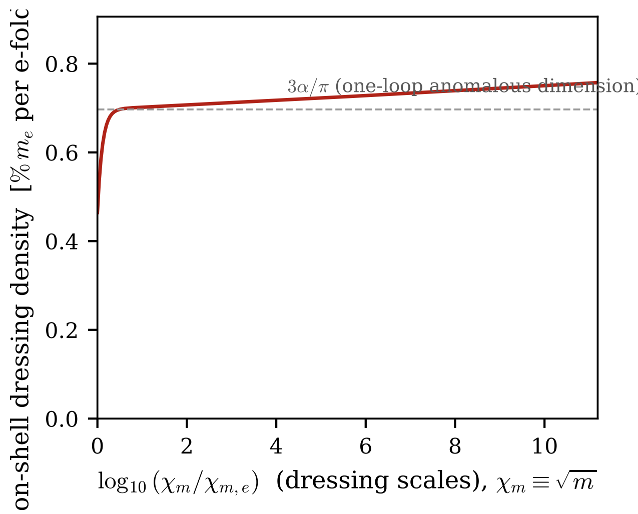

FIG. 3. The electron's mass-budget density across dressing scales (one loop, on-shell projection, running α). The plateau equals the QED anomalous dimension exactly; eleven decades of χ_m carry a scale-invariant $1/\chi_m$ measure, broken only at the Compton scale.

VII. FLAVOR STRUCTURE

Permutations of the three family modes give the S_3 decomposition used by the Koide/equipartition construction. Allowing signed square roots enlarges the *configuration space* and organizes sign choices under the signed-permutation group $B_3 = S_3 \ltimes \mathbb{Z}_2^3$. The latter should not be described as a symmetry of the Koide ratio itself, because independent sign flips change $(\sum_i \chi_{m,i})^2$ in general. The companion paper establishes the S_3 equipartition formulation and uses the B_3 action as a classification of signed neutrino configurations; we adopt that more precise language here.

One further empirical layer belongs to the third moment $p_3 = \sum \chi_{m,i}^3$, which selects the point on the Koide circle (the individual masses). In the Koide–Brannen parametrization $\sqrt{m_k} = \mu[1 + \sqrt{2}\cos(2\pi k/3 + \delta)]$ the current data give [C]

$$\delta_\ell = 0.22223 \pm 0.00002 \quad (\tfrac{2}{9}:\ +0.4\sigma),$$
$$\delta_\nu - \delta_\ell = 0.25703 \pm 0.00376 \quad (\tfrac{\pi}{12}:\ -1.3\sigma), \tag{36}$$

confirming on 2024–26 inputs the regularities noted by Brannen [15]. We record, with a [D] label and without elaboration, that the construction now carries three candidate angles – $\delta_\ell = 2/9$, $\Delta\delta = \pi/12$, and the flux $a \approx \pi/18$ – inviting the question of a common discrete structure.

VIII. COSMOLOGY: A NEGATIVE RESULT AND A CONJECTURE

Coupling the vacuum energy directly to the coordinate of a single mode, $\rho_q \propto 1/\eta^p$ with $p = 2q$, is excluded at the background level: anchoring the matter density at recombination, the acoustic scale θ^* forces parameters that degrade the BAO fit catastrophically ($\Delta\chi^2 \approx +137$ for $p = 2$, $+39$ for $p = 1$, relative to ΛCDM against DESI DR2 [25]), with the data pulling $p \to 0$, i.e. toward a constant [B]. We state the failure plainly: the vacuum does not couple to the coordinate of a single mode. The framework's conjecture [D] is structural instead: if masses are diagonal variances of a mode covariance matrix and interactions its off-diagonal entries, the vacuum energy is the sum of *all* variances with covariances – a quantity that the same off-diagonal structure which produces the covariance ladder of [1] can freeze to a quasi-constant – supplemented by the constant rotational term $-I\Omega^2/2$ of Sec. V. Both statements are conjectures, so labeled.

IX. FALSIFICATION SCHEDULE

Table IV separates direct tests from conditional signatures. A formal level location is not by itself an experimental prediction until the model also specifies the coupling or mixing through which the level can be produced and observed.

X. DISCUSSION

Table V condenses the framework into its working principles: *two postulates, eleven consequences, one diagnostic*. Everything below the postulates carries a proof, a number with a pull, or an explicit hypothesis label; and the two no-go theorems (integer ladders; fractional dimensions) show the framework killing its own most tempting readings – a pattern we regard as its principal methodological credential.

The framework's relations to the literature are each a single, sharp difference. From Wesson's Space-Time-Matter [5, 6] it differs only in the dictionary, with a factor-two observable consequence. From zitterbewegung models [12–14] it inherits the circulation identity $E = mc^2$ but places the circulation on an SQUS loop in the ordinary three-dimensional sector, whose size is controlled by the fifth coordinate. The quadratic horn gives an inner barrier; stability requires a radial completion satisfying Eqs. (25) and (26). The holonomy is a closed-loop $U(1)$ phase structure fitted conditionally to neutrino mass ratios; its rotational reading is limited by the Sagnac equivalence [19]. A single outlook sentence [D]: a rotating background that favors one handedness invites examination as a geometric root of parity violation in the weak sector.

TABLE IV. Direct tests and conditional signatures. The neutrino mass sums and $m_{\beta\beta}$ bands are branch-dependent results of the companion construction. Formal winding levels are conditional until their mixings and population rules are derived.

Observable	Prediction / condition	Test
mass ordering	selects NO or IO branch	JUNO [26]
Σm_ν	59.16(24) meV (NO); 102.0(4) meV (IO)	cosmology*
$m_{\beta\beta}$	1.3–4.0 meV (NO); 18–48 meV (IO)	$0\nu\beta\beta$
residual drift	leakage from $V_{\rm rad}$	clock programs
SQUS stability	$h(\xi_*) = 1$, $h'(\xi_*) < 0$	internal theore
$\ell = 4$ level	166.7 meV if populated and mixed	conditional
$\ell = 0, -1, -2$	formal level locations only	conditional
Koide floor	$\lvert Q - \frac{2}{3}\rvert \sim 10^{-6}$	Belle II

*Cosmological interpretation is model-dependent; a quoted mass-sum bound must specify the cosmological model.

Limitations, stated plainly: the absolute radial stabilizer has not yet been derived microscopically; the pure quadratic horn is a barrier, not a stable orbit; the scalar SQUS construction does not yet derive spin 1/2; the identification of radial eigenvalues with $\sqrt{m}$ remains a spectral postulate to be derived from a field equation; the winding extension does not yet predict mixings or population rules for additional levels; the electron profile is one-loop and its detailed mass-budget split is scheme-dependent; the spectral-curve fit has weak selective power on its own; the flux/rotation degeneracy is an epistemic boundary; and entries labeled [C] and [D] are regularities and hypotheses, not results. The framework survives, in the end, exactly as far as Table IV permits it to.

Appendix A: Geodesic and SQUS reductions

For the canonical metric (6), define the 4D proper interval by $ds^2 = g_{\mu\nu}dx^\mu dx^\nu$. The null condition is

$$0 = \frac{\xi^2}{L^2}ds^2 - d\xi^2, \tag{A1}$$

TABLE V. The principles of the framework. Status labels as in the text: [A] theorem/exact, [B] computation vs. data, [C] empirical regularity, [D] postulate/hypothesis.

Principle	Content	Status	Se
Postulates			
P1 square-root coordinate	$\chi_m = \sqrt{m}$ maps to the dimensionful fifth coordinate $\xi = \kappa\chi_m$	[D]	I
P2 SQUS circulation	a stable particle may support coherent circulation in ordinary 3-space on an SQUS orbit	[D]	IV
Kinematics and conservation			
P3 master decomposition	$m = \bar{\chi}_m^2 + \mathrm{Var}(\chi_m)$ exact by definition; SM mapping interpretive	[A/D]	II
P4 causal budget	$v_3^2 + w_\xi^2 = c^2$ exactly; CM/circulation split is an ansatz	[A/D]	II
P5 cost of scale travel	free null motion gives one e-fold of ξ per L/c; observed drift requires radial stabilization	[A/B]	II
P6 sharpness of stable modes	$\Delta\chi_m = \Gamma/(2c^2\sqrt{m})$; stable mode $\Rightarrow$ sharp mass coordinate	[A]	II
P7 geometric homogeneity	identical fifth-coordinate/SQUS structure over every base point; quasar spectroscopy, 10^{-5}–10^{-7}	[B]	II
Dynamics and spectrum			
P8 equipartition	$Q = \frac{2}{3} \iff \boldsymbol{n_1} = \boldsymbol{n_2}$; V_{eq} fixes family direction, not radial scale	[A/B]	VI
P9 SQUS stability	single-scale warp gives $f \propto \xi^2$ near tip; orbit $h = 1$; stable if $h' < 0$	[A/D]	IV
P10 winding closure	integer winding numbers; ratios bounded by concavity absent a twist	[A/B]	V
P11 background twist	within separable $U(1)$ ansatz, $\varepsilon_\ell \propto (\ell - a)^2$, $a = 0.1726(68)$	[B/D]	V
Scaling			
P12 scaling signatures	log-uniform spectrum, quasi-frozen Q, and RG dressing show related scale structure	[B]	V
P13 criticality of the tip	$\xi = 0$ as a conjectured critical limit; $1/\xi^2$ is scale free	[D]	V
Diagnostic			
D1 surface tension	$\sigma = \frac{3}{8\pi} m^3 c^4/\hbar^2 = \frac{3}{8\pi}\chi_m^6 c^4/\hbar^2$: a 44-decade ladder, zero at the sphere	[B/C]	II

which immediately gives $d\xi/ds = \pm\xi/L$. This is the clean derivation of Eq. (8); no additional normalization of the warped 4D term is imposed.

To describe an SQUS circulation without adding a sixth dimension, use ordinary spatial coordinates adapted to the orbit. A reduced sector of the five-dimensional geometry can be written as

$$dS_{\mathrm{red}}^2 = \frac{\xi^2}{L^2}(dt^2 - dz^2) - B(\xi)d\xi^2 - f(\xi)^2 d\varphi^2, \tag{A2}$$

where φ is an ordinary azimuthal angle. With affine parameter λ and dots meaning $d/d\lambda$,

$$E = (\xi/L)^2\dot{t}, \qquad p = (\xi/L)^2\dot{z}, \qquad J = f^2\dot{\varphi}. \tag{A3}$$

The null condition gives

$$B(\xi)\dot{\xi}^2 = \frac{L^2(E^2 - p^2)}{\xi^2} - \frac{J^2}{f(\xi)^2}, \tag{A4}$$

which is Eq. (23). A proper radial coordinate $d\rho = \sqrt{B}\,d\xi$ sets the kinetic coefficient to unity locally. For $B = 1$,

$$\ddot{\xi} = -\frac{A}{\xi^3} + \frac{J^2 f'(\xi)}{f(\xi)^3}. \tag{A5}$$

Combining $\dot{\xi} = 0$ and $\ddot{\xi} = 0$ yields $f'/f = 1/\xi$, i.e. Eq. (25). For the quadratic horn $f = \xi^2/R_s$, the root of $\dot{\xi} = 0$ is the turning point $\xi_t^2 = J^2R_s^2/A$, and $\ddot{\xi}(\xi_t) = A/\xi_t^3 > 0$.

For the effective two-dimensional SQUS configuration metric $d\rho^2 + f(\rho)^2 d\varphi^2$, separation in ordinary azimuthal modes $e^{i\ell\varphi}$ produces the radial term ℓ^2/f^2. The Liouville substitution $u = v/\sqrt{f}$ yields the Schrödinger form with potential $\ell^2/f^2 + f'^2/(4f^2) - f''/(2f)$. The spectral analysis therefore concerns an effective SQUS configuration sector, not an additional spacetime dimension.

Appendix B: Two no-go theorems

1. No integer ladders on the cone

Seek integer triples $(1, a, b)$ with $Q = \frac{2}{3}$ in either sign class: $3(1 + a^2 + b^2) = 2(\pm 1 + a + b)^2$. Reduction gives the requirement that $3(b^2 \mp 4b + 1)$ be a perfect square; writing $b \mp 2 = 3j$ this becomes $k^2 \equiv 2 \pmod 3$, impossible since squares mod 3 are $\{0, 1\}$. Hence no integer χ_m-ladder normalized to its lightest member lies on the equipartition cone. $\square$

2. Concavity bound for horn spectra

Let $H(\lambda) = H_0 + \lambda U$ with $U \geq 0$, $\lambda = \ell^2$, on any radial domain with any self-adjoint closure. The ground eigenvalue $\varepsilon(\lambda) = \inf_\psi \langle\psi|H(\lambda)|\psi\rangle$ is an infimum of affine functions of λ, hence concave; with $\varepsilon(0) \geq 0$, Jensen's inequality between 0 and 4λ (and 9λ) gives $\varepsilon(4\lambda) \leq 4\varepsilon(\lambda)$ and $\varepsilon(9\lambda) \leq 9\varepsilon(\lambda)$, i.e. Eq. (31). A holonomy evades the theorem because it shifts $\ell \to \ell - a$ rather than scaling the same nonnegative U. The statement is limited to this operator class. □

Appendix C: Fits and error propagation

The cone ratios $r_{2,3}$ are Monte-Carlo propagated from $\Delta m^2_{21} = 7.49(19) \times 10^{-5}$ eV^2 and $\Delta m^2_{31} = 2.513(21) \times 10^{-3}$ eV^2 [16] through the exact cone solution. Spectral families are fitted to r_2 by root finding and judged on the predicted r_3; the flux uncertainty follows from $\sigma_a = \sigma_{r_2} |da/dr_2|$. The mass-measure fit is a truncated-Pareto maximum likelihood on the nine charged-fermion masses with both endpoints fixed at the observed range. All analysis scripts are public (Data Availability).

DATA AVAILABILITY

All analysis scripts reproducing the tables, figures and numerical results of this work are publicly available at [repository/Zenodo DOI].

[1] K. Urbanowicz, "Equipartition interpretation of the Koide relation: representation-theoretic formulation, covariance test, and neutrino mass predictions," DOI: 10.5281/zenodo.21325642.

[2] Y. Koide, "Fermion-boson two-body model of quarks and leptons and Cabibbo mixing," Lett. Nuovo Cim. **34**, 201 (1982).

[3] Y. Koide, "A fermion-boson composite model of quarks and leptons," Phys. Lett. B **120**, 161 (1983).

[4] S. Navas *et al.* (Particle Data Group), "Review of Particle Physics," Phys. Rev. D **110**, 030001 (2024).

[5] P. S. Wesson and J. Ponce de Leon, "Kaluza-Klein equations, Einstein's equations, and an effective energy-momentum tensor," J. Math. Phys. **33**, 3883 (1992).

[6] J. M. Overduin and P. S. Wesson, "Kaluza-Klein gravity," Phys. Rept. **283**, 303 (1997), arXiv:gr-qc/9805018.

[7] B. Mashhoon, H. Liu and P. S. Wesson, "Particle masses and the cosmological constant in Kaluza-Klein theory," Phys. Lett. B **331**, 305 (1994).

[8] M. J. Duff, "Comment on time-variation of fundamental constants," arXiv:hep-th/0208093.

[9] N. Huntemann *et al.*, "Improved limit on a temporal variation of m_p/m_e from comparisons of Yb$^+$ and Cs atomic clocks," Phys. Rev. Lett. **113**, 210802 (2014).

[10] W. Ubachs *et al.*, "Search for a drift of the proton-electron mass ratio," Rev. Mod. Phys. **88**, 021003 (2016).

[11] E. V. Pitjeva and N. P. Pitjev, "Estimates of changes of the Sun's mass and the gravitational constant from planetary ephemerides," Mon. Not. Roy. Astron. Soc. **432**, 3431 (2013).

[12] E. Schrödinger, "Über die kräftefreie Bewegung in der relativistischen Quantenmechanik," Sitz. Preuss. Akad. Wiss. Phys.-Math. Kl. **24**, 418 (1930).

[13] D. Hestenes, "The zitterbewegung interpretation of quantum mechanics," Found. Phys. **20**, 1213 (1990).

[14] R. Penrose, *The Road to Reality* (Jonathan Cape, London, 2004), Ch. 25.

[15] C. A. Brannen, "The lepton masses," preprint (2006), http://brannenworks.com.

[16] I. Esteban *et al.*, "NuFit-6.0: updated global analysis of three-flavor neutrino oscillations," JHEP **12**, 216 (2024), arXiv:2410.05380; www.nu-fit.org.

[17] Y. Aharonov and D. Bohm, "Significance of electromagnetic potentials in the quantum theory," Phys. Rev. **115**, 485 (1959).

[18] Y. Hosotani, "Dynamical mass generation by compact extra dimensions," Phys. Lett. B **126**, 309 (1983).

[19] G. Sagnac, "L'éther lumineux démontré par l'effet du vent relatif d'éther dans un interféromètre en rotation uniforme," C. R. Acad. Sci. **157**, 708 (1913).

[20] Ya. B. Zel'dovich, "Generation of waves by a rotating body," JETP Lett. **14**, 180 (1971).

[21] J. L. Friedman, "Ergosphere instability," Commun. Math. Phys. **63**, 243 (1978).

[22] V. Efimov, "Energy levels arising from resonant two-body forces in a three-body system," Phys. Lett. B **33**, 563 (1970).

[23] D. Buchholz, "Gauss' law and the infraparticle problem," Phys. Lett. B **174**, 331 (1986).

[24] G. Jona-Lasinio, "The renormalization group: a probabilistic view," Nuovo Cim. B **26**, 99 (1975).

[25] M. Abdul Karim *et al.* (DESI Collaboration), "DESI DR2 Results II: Measurements of Baryon Acoustic Oscillations and Cosmological Constraints," Phys. Rev. D **112**, 083515 (2025), arXiv:2503.14738.

[26] A. Abusleme *et al.* (JUNO Collaboration), "First measurement of reactor neutrino oscillations at JUNO," arXiv:2511.14593.